
A Kernel Two-sample Test for Dynamical Systems

Friedrich Solowjow¹ Dominik Baumann^{1,2} Christian Fiedler^{1,2} Andreas Jocham³ Thomas Seel⁴
Sebastian Trimpe^{1,2}

Abstract

Evaluating whether data streams were generated by the same distribution is at the heart of many machine learning problems, e.g., to detect changes. This is particularly relevant for data generated by dynamical systems since they are essential for many real-world processes in biomedical, economic, or engineering systems. While kernel two-sample tests are powerful for comparing independent and identically distributed random variables, no established method exists for comparing dynamical systems. The key problem is the critical independence assumption, which is inherently violated in dynamical systems. We propose a novel two-sample test for dynamical systems by addressing three core challenges: we (i) introduce a novel notion of mixing that captures autocorrelations in a relevant metric, (ii) propose an efficient way to estimate the speed of mixing purely from data, and (iii) integrate these into established kernel-two sample tests. The result is a data-driven method for comparison of dynamical systems that is easy to use in practice and comes with sound theoretical guarantees. In an example application to anomaly detection from human walking data, we show that the test readily applies without the need for feature engineering, heuristics, and human expert knowledge.

1. Introduction

Comparing dynamical systems is a relevant problem in many domains. For instance, modern engineering applications often leverage computer simulations instead of directly interacting with the physical plant since real experiments are

more expensive, time consuming, and cause wear on the hardware. Besides, being able to predict the response of a physical plant based on a mathematical model enables powerful learning algorithms (Hwangbo et al., 2019), model-predictive control (Qin & Badgwell, 2003), and digital twins in future manufacturing (Jeschke et al., 2017). The success of these methods, however, is critically intertwined with the model accuracy. Thus, it is essential to ensure accurate models, for example, by comparing data generated from the simulation model with data collected from the real system. For biomedical systems such as the human cardiovascular system, central nervous system, or musculoskeletal system, implementing a principled comparison of systems at different time instances can help to detect diseases or quantify their severity. For example, pathologies in human gaits can be indicators for early signs of Parkinson’s disease (Nguyen et al., 2019). Thus, an algorithm that automatically compares new data to labeled records could help physicians in their decision making.

Despite its practical relevance, there is no established way of comparing dynamical systems in general. For complex processes that are difficult to model, even data-driven approaches typically require expert knowledge. In biomedical systems, for example, when expressive features are available, successful detection of spasticities has been achieved (Misgeld et al., 2015; Lueken et al., 2015). But clearly, the success of this approach critically depends on the expressiveness of these features and on how well the problem is understood. A related and seemingly straightforward approach may involve the identification and subsequent comparison of dynamical system models or other intermediate objects. However, this will inevitably introduce a model bias. Further, nonlinear dynamical systems are cumbersome to model and often difficult to learn (cf. examples presented in Brunton et al. (2017); Ljung (2001)).

We propose a kernel two-sample test for comparing dynamical systems. The test is purely data-driven and does not require any feature engineering, human expert knowledge, or heuristics. We leverage modern kernel techniques to compare the underlying stationary distributions of dynamical systems. However, instead of first estimating the distributions and then comparing them, the test directly operates on the raw data generated by the dynamical system such as

¹Intelligent Control Systems Group, Max Planck Institute for Intelligent Systems, Stuttgart, Germany ²Institute for Data Science in Mechanical Engineering, RWTH Aachen University, Aachen, Germany ³Institut Physiotherapie, FH JOANNEUM, Graz, Austria ⁴Control Systems Group, Technische Universität Berlin, Berlin, Germany. Correspondence to: Friedrich Solowjow <solowjow@is.mpg.de>.

sensor measurements or simulations. This yields a statistical test with theoretical guarantees and meaningful assumptions on when it is applicable and when not. Further, our test can straightforwardly be used since it is built upon standard implementations of kernel-based algorithms.

While we can exploit parts of existing kernel-based results, and especially their theoretical guarantees, the extension to comparing dynamical systems is not straightforward. This is mainly because kernel two-sample testing was initially developed for independent and identically distributed (i.i.d.) random variables (Gretton et al., 2012a). The test approximates a metric on the space of probability distributions (the maximum mean discrepancy (MMD)) through kernel-based techniques. Due to its powerful theoretical properties and versatile applicability, kernel-two sample testing is a well established and prominent method in the machine learning community (Long et al., 2017; Tolstikhin et al., 2018; Muandet et al., 2017; Schölkopf & Smola, 2001). The i.i.d. assumption in the test is critical, but it is violated by the very nature of dynamical systems: through the dynamics samples at time t are coupled to previous and future samples. To address this issue, we introduce a novel notion of mixing that considers the dependence of data through time with respect to the MMD. Intuitively, mixing reveals how fast autocorrelations decay and, thus, how long we need to wait in-between samples for data to be (approximately) independent. Our new mixing notion can be efficiently estimated from data and is particularly synergistic with kernel two-sample tests since both measure distances of probability distributions with respect to the same metric – the MMD. By estimating the decay of dependency and embedding this into well-established algorithms, we obtain a powerful test for comparing dynamical systems.

To make kernel two-sample testing amenable to dynamical systems, we quantify and estimate the speed of mixing. This is an important contribution in itself also beyond the proposed test, because it allows for generalizing theorems from the i.i.d. setting to more general problems (Yu, 1994). In most existing literature, the decay of autocorrelations is bounded a priori by assumption (Chwialkowski & Gretton, 2014). However, there can easily be a drastic mismatch between what is postulated in order to prove theoretical results and the actual properties of the system. Determining mixing properties of dynamical systems is an active field of research (Chazottes, 2015; Hang et al., 2017), and standard mixing properties may well be violated for certain classes of dynamical systems (Simchowitz et al., 2018). Thus, it is questionable to impose such mixing requirements a priori without proper justification. By estimating mixing rates from data, we obtain sharp tests that are tailored to the considered systems. Surprisingly, there is only very limited work that addresses the estimation of mixing coefficients from data, as also acknowledged and emphasized in (Mc-

Donald et al., 2011). The approach proposed in (McDonald et al., 2011) is different from our work, as mixing is considered with respect to the total variation norm, which requires the estimation of complex intermediate objects while we estimate mixing properties directly from data.

By combining the estimation of mixing properties with kernel-based techniques, we obtain a powerful statistical test for comparing dynamical systems. We demonstrate the efficiency and robustness of the proposed test numerically and on experimental data. In particular, we consider human walking experiments and analyze raw data from an inertial measurement unit (IMU) to detect anomalies in the walking pattern. Without the need for human expert knowledge or fitting model parameters, our test outperforms standard baselines in deciding which of the trajectories were generated with an attached knee orthosis.

Contributions: We propose a kernel two-sample test for dynamical systems. By developing a new notion of mixing that can be estimated from data, we generalize powerful theoretical guarantees from the i.i.d. setting to dynamical systems. The derived method is straightforward to use, and well-established implementations of the kernel two-sample test can be leveraged. We demonstrate the robustness and efficiency of the method on real-world data, where we achieve better results than standard baselines, without relying on feature engineering or expert knowledge. Code and data will be made available upon publication.

2. Related Work

There is only limited literature that explicitly investigates the question of how to compare dynamical systems. One possibility is the embedding of dynamical systems as infinite-dimensional objects into reproducing kernel Hilbert spaces (RKHS) with specifically designed kernels such as Binet-Cauchy kernels (Vishwanathan et al., 2007) or generalizations thereof as proposed in Ishikawa et al. (2018) and Ishikawa et al. (2019). A similar function-analytical approach is considered in Mezić (2016) and Klus et al. (2020), where the authors consider Koopman and Perron-Frobenius operators to obtain linear dynamics in an infinite-dimensional space. These articles leverage specifically designed kernels and linear operators associated with dynamical systems to obtain an embedding. However, none of the above articles proposes a statistical test that compares dynamical systems. This would require further finite sample and error bounds on the approximations of the infinite dimensional operators, which is far from trivial.

The critical technical issue when dealing with dynamical systems is non-i.i.d. data. There are several extensions of kernel two-sample tests that have been developed (Zaremba et al., 2013; Gretton et al., 2012b; Doran et al., 2014;

Lloyd & Ghahramani, 2015; Chwialkowski et al., 2014; Chwialkowski & Gretton, 2014) to make them applicable to a broader range of problems, where non-i.i.d. data is also an issue. However, the strong mixing properties that are typically postulated limit the applicability of the results to dynamical systems. Instead of *assuming* such properties, we propose a novel mixing notion that ideally fits the kernel-two sample test and that can be *estimated* from data (in contrast to most other mixing notions).

The problem of comparing dynamical systems is also present in control theory and was, for example, recently studied in (Umlauf & Hirche, 2019; Solowjow & Trimpe, 2020) considering the question of when to trigger model updates. In robust control, there is the notion of the gap metric (Zhou & Doyle, 1998), which compares the closed-loop behavior of dynamical systems. These approaches are particularly promising to quantify the similarities between dynamical systems when trying to achieve effective transfer learning, as shown in (Sorocky et al., 2020). However, they usually rely on a given model and a certain linear structure in the system. Depending on the prior system information, there exist more model-based approaches that compare dynamical systems. But estimating such models of nonlinear systems can be difficult in practice (Schoukens & Ljung, 2019; Schön et al., 2011). Similarly, estimating the stationary measure of a dynamical system is also a highly nontrivial problem (Hang et al., 2018; Luzzatto et al., 2005). In our approach, we do not require any intermediate objects. Instead, we compare dynamical systems directly from data.

3. Assumptions and Problem Formulation

In the following, we introduce the mathematical objects that we will consider in this paper. Afterward, we make the problem explicit.

3.1. Stationary and Ergodic Systems

Let (Ω, \mathcal{A}, P) be a probability space, $S \subset \mathbb{R}^d$ a compact set, which is the state space of the dynamical system, and \mathcal{B} the corresponding Borel σ -algebra. We define a stochastic dynamical system $\{X_k\}$ as a collection of random variables indexed in discrete time $k \in \mathbb{N}$ and $X_k: \Omega \rightarrow S$. We assume that the system X_k is ergodic and stationary.

Definition 1 (Stationary). *A system is stationary if the joint distribution of its states is invariant with respect to arbitrary time shifts for any collection of sampling instances.*

In addition to stationary behavior, we also require ergodicity. While stationarity ensures time-invariant distributions, ergodicity guarantees that the statistical properties of the system do not differ over multiple realizations. We use a standard definition that goes back to (Birkhoff, 1931).

Definition 2 (Ergodic). *Assume the system $\{X_k\}$ is station-*

ary with distribution \mathbb{P} . We call the system ergodic if for all $\phi \in L^1_{\mathbb{P}}(S)$ and \mathbb{P} -almost all initial states we have

$$\lim_{N \rightarrow \infty} \frac{1}{N} \sum_{k=0}^{N-1} \phi(X_k) = \int_S \phi(y) d\mathbb{P}(y). \quad (1)$$

Equation (1) is in some sense a realization of the law of large numbers, and both sides of the equation yield the expected value $\mathbb{E}_{\mathbb{P}}[\phi]$. In particular, it allows us to estimate $\mathbb{E}[X_k]$ (the distribution is invariant for all k) from long enough sample paths.

Many practical systems satisfy the above assumptions, or can be approximated as such. An important special case that we will investigate in detail are state-space models or Markov chains with continuous state spaces of the type $X_{k+1} = f(X_k) + \epsilon_k$, where f is an appropriate dynamics function and ϵ_k the process noise. This system description is highly relevant in systems and control theory. Further, we will also consider chaotic systems, where $\epsilon_k \equiv 0$. These are deterministic and violate common probabilistic mixing assumptions.

3.2. Problem Formulation

Consider two stationary and ergodic systems $\{X_k\}$ and $\{Y_k\}$ with stationary distributions \mathbb{P}_X and \mathbb{P}_Y . The problem that we investigate in this paper is to decide whether two data streams $X = \{X_0, X_1, \dots, X_n\}$ and $Y = \{Y_0, Y_1, \dots, Y_n\}$ were generated by different (unknown) systems. We assume $X_i, Y_i \in S$ and, in general, $X_0 \neq Y_0$. Further, we assume that the dynamical systems have converged to their stationary distribution, and we do not consider any transients.

We propose to compare dynamical systems by investigating their stationary probability measures. Thus, we obtain the null hypothesis

$$H_0: \mathbb{P}_X = \mathbb{P}_Y, \quad (2)$$

which we try to reject with high confidence. For our method, it is not necessary to estimate or construct any intermediate objects such as the dynamics function f , nor the measures \mathbb{P}_X and \mathbb{P}_Y . Here, we consider a two-sample setting between two data streams X and Y . However, this can easily be applied to settings where we want to investigate whether a given model coincides with reality. Then, samples obtained through sensor measurements can be compared with samples generated from the model.

4. Technical Preliminaries

The main idea of this paper can be summarized as generalizing kernel two-sample tests (Gretton et al., 2012a) to dynamical systems. Essentially, we propose to wait *long enough* between consecutive samples, which is made precise

in Sec. 5.2. Thus, enforcing negligibly small autocorrelations and, therefore, recovering the i.i.d. setting. We begin by summarizing key results from kernel two-sample tests and kernel mean embeddings.

4.1. Kernel Two-sample Test

An elegant and efficient comparison of probability distributions can be achieved with kernel two-sample tests (Gretton et al., 2012a). The distributions are embedded into an RKHS, where it becomes tractable to compute certain metrics on the space of probability distributions such as the MMD. The following definitions and theorems are taken from Gretton et al. (2012a).

Definition 3 (MMD). *Let (S, d) be a metric space and let $\mathbb{P}_X, \mathbb{P}_Y$ be two Borel probability measures defined on S . Further, let \mathcal{F} be the unit ball in an RKHS on S . We define the maximum mean discrepancy*

$$\text{MMD}^2[\mathbb{P}_X, \mathbb{P}_Y] = \sup_{g \in \mathcal{F}} (\mathbb{E}_{\mathbb{P}_X}[g] - \mathbb{E}_{\mathbb{P}_Y}[g])^2. \quad (3)$$

The MMD yields a semi-metric between probability distributions and can be efficiently estimated by embedding the distributions into an RKHS \mathcal{H} with the aid of kernel mean embeddings (Muandet et al., 2017). It is a challenging problem to compute (3) directly since \mathcal{F} is usually infinite-dimensional. However, by kernelizing this problem, it is possible to estimate (3) from data.

Theorem 1. *Assume k is a characteristic kernel and \mathcal{F} is the unit ball in the corresponding RKHS \mathcal{H} . Further, assume (X_1, \dots, X_n) and (Y_1, \dots, Y_m) are drawn i.i.d. from \mathbb{P}_X respectively \mathbb{P}_Y . Then, we obtain the following estimate*

$$\begin{aligned} \text{MMD}_b^2[\mathbb{P}_X, \mathbb{P}_Y] &= \frac{1}{n^2} \sum_{i,j=1}^n k(X_i, X_j) + \\ &\frac{1}{m^2} \sum_{i,j=1}^m k(Y_i, Y_j) - \frac{2}{mn} \sum_{i=1}^n \sum_{j=1}^m k(X_i, Y_j). \end{aligned} \quad (4)$$

The requirement of a characteristic kernel ensures that the embedding of the probability distribution is injective and, thus, a metric is obtained. The kernel k can, for example, be chosen as a Gaussian kernel since it is well known to be characteristic (Steinwart & Christmann, 2008).

Theorem 2. *Assume k is a characteristic kernel and \mathcal{F} is the unit ball in the corresponding RKHS \mathcal{H} . Then $\text{MMD}^2[\mathbb{P}_X, \mathbb{P}_Y] = 0$ if, and only if, $\mathbb{P}_X = \mathbb{P}_Y$.*

Essentially, we do not require any prior knowledge or parameterization of \mathbb{P}_X and \mathbb{P}_Y . Access to i.i.d. samples from these distributions is enough. In practice, we only consider finitely many data points and, thus, an estimate of the MMD. This estimate is expected to have some deviation, i.e., even

for identical distributions, the test statistic will be larger than zero. Therefore, we need finite sample bounds that quantify the convergence speed of the empirical MMD to obtain confidence bounds. These bounds are usually the reason for the i.i.d. assumption and yield thresholds κ .

4.2. Hilbert-Schmidt Independence Criterion

The Hilbert-Schmidt independence criterion (HSIC) (Gretton et al., 2008) quantifies dependence between random variables. Generally, two random variables X and Y are independent if their joint distribution factorize, i.e., $\mathbb{P}_{X,Y} = \mathbb{P}_X \otimes \mathbb{P}_Y$, where \otimes denotes the tensor product. Estimating the involved objects from data is usually intractable. Thus, we consider the HSIC based on

Definition 4 (HSIC, Sejdinovic et al. (2013, Def. 11)). *Let $X \sim P_X$ and $Y \sim P_Y$ be random variables with joint distribution $P_{X,Y}$. The HSIC is defined as*

$$\text{HSIC}(X, Y) = \|P_X \otimes P_Y - P_{X,Y}\|_{\text{MMD}}. \quad (5)$$

Similar as for the kernel two-sample test, it is possible to express (5) in terms of kernel evaluations. Further, it is also possible to provide high confidence bounds and thus, obtain an efficient statistical test for i.i.d. data.

The general framework is highly flexible and can deal with a variety of objects. For our problem, we can use a simplified setting, which coincides with the setup for the kernel two-sample test. Estimations of (5) in terms of kernel evaluations can be found in (Gretton et al., 2008, Equation (4)).

5. Two-sample Test for Dynamical Systems

In order to extend the kernel two-sample test to dynamical systems, we need to address the autocorrelations inherent in the data. Effectively, concentration results quantify the uncertainty due to random effects and answer the question of how much data is needed to make high confidence decisions. Autocorrelations void these results to some extent, as we demonstrate in our illustrative example (cf. Fig. 1). However, by estimating the autocorrelations within the process and acting accordingly, we can recover the standard results.

5.1. Decay of Autocorrelations

There are various types of mixing that essentially all describe the decay of autocorrelations. They are notoriously difficult or even impossible to estimate, and many types of mixing do not apply to large classes of dynamical systems (Hang et al., 2017). We propose a novel type of mixing that can be estimated from data and yields advantageous theoretical properties. We start with introducing β -mixing similarly as in (McDonald et al., 2011):

$$\beta(a) = \sup_s \|\mathbb{P}_{-\infty}^s \otimes \mathbb{P}_{s+a}^\infty - \mathbb{P}_{s,a}\|_{\text{TV}}, \quad (6)$$

where $\mathbb{P}_{-\infty}^s$ is the joint distribution of the states $\{X_t\}_{t=-\infty}^s$ and \mathbb{P}_{s+a}^∞ of $\{X_t\}_{t=s+a}^\infty$. With $\mathbb{P}_{s,a}$ we denote the joint distribution of the objects around the tensor sign, here $(\{X_t\}_{t=-\infty}^s, \{X_t\}_{t=s+a}^\infty)$ and use $\|\cdot\|_{\text{TV}}$ for total variation. The process is β -mixing if $\beta(a) \rightarrow 0$ for $a \rightarrow \infty$. In McDonald et al. (2011), the coefficient is estimated through involved density estimations, and the authors emphasize that they solve a more difficult problem to obtain a solution to a simpler one.

We propose a direct estimation method for a weaker (i.e., less restrictive) type of mixing.

Definition 5 (MMD-mixing). We call a process MMD-mixing if $\|\mathbb{P}_0^s \otimes \mathbb{P}_{s+a}^{2s+a} - \mathbb{P}_{s,a}\|_{\text{MMD}} \rightarrow 0$ for $a \rightarrow \infty$.

Due to stationarity, we can omit the supremum. Further, we slightly abuse the $\mathbb{P}_{s,a}$ notation and restrict ourselves to distributions of finite length s for an efficient estimation. MMD-mixing is compatible with the standard notion of β -mixing and yields lower bounds:

Lemma 1. A β -mixing process is MMD-mixing for any bounded kernel.

Proof. This property follows by considering Hilbert space embeddings of probability distributions. In particular, Sriperumbudur et al. (2010, Theorem 21 (iii)) shows that

$$\|\mathbb{P} - \mathbb{Q}\|_{\text{MMD}} \leq C \|\mathbb{P} - \mathbb{Q}\|_{\text{TV}}, \quad (7)$$

where C is the supremum of the corresponding kernel. \square

The other direction does not always hold. For instance, deterministic dynamical systems are, in general, not β -mixing (Hang et al., 2017). However, recent results show that convergence in MMD metrizes weak convergence in the space of probability distributions (Simon-Gabriel et al., 2020). Thus, convergence in MMD is applicable to discrete data and Dirac distributions. This is particularly relevant when considering mixing properties of deterministic dynamical systems.

Definition 5 is conceptually based on β -mixing and considers joint distributions of subtrajectories. In practice, however, it is usually sufficient to consider data from two points in time \mathbb{P}_s and \mathbb{P}_{s+a} . In particular, when kernel two-sample testing is also based on points and not subtrajectories.

Definition 6 (Weak MMD-mixing). We call a process weak MMD-mixing if $\|\mathbb{P}_s \otimes \mathbb{P}_{s+a} - \mathbb{P}_{s,a}\|_{\text{MMD}} \rightarrow 0$ for $a \rightarrow \infty$.

5.2. Estimating MMD-mixing

For clarity of presentation, we start with the estimation of weak MMD-mixing (Def. 6), which we also consider in our numerical experiments. To estimate the mixing

properties of a system, we assume access to m independent trajectories. In this setting, we can apply the HSIC (5). We pick two points from each trajectory, $X_s^{(i)}$ and $X_{s+a}^{(i)}$. Due to stationarity, the time s does not matter. We divide the data into $X_s = \{X_s^{(1)}, X_s^{(2)}, \dots, X_s^{(m)}\}$ and $X_{s+a} = \{X_{s+a}^{(1)}, X_{s+a}^{(2)}, \dots, X_{s+a}^{(m)}\}$. The sets are, per construction, i.i.d. within themselves. Next, we can compute $\text{HSIC}(X_s, X_{s+a})$ and iteratively increase a . If we pick a large enough, the HSIC will eventually become arbitrarily small. In particular, weak MMD-mixing gives us that $\text{HSIC}(X_s, X_{s+a}) \rightarrow 0$ for $a \rightarrow \infty$. For practical algorithms, we will fix a small $\epsilon > 0$ and enforce $\text{HSIC}(X_s, X_{s+a^*}) < \epsilon$. In our experiments, we pick ϵ as the standard test threshold of the HSIC (cf. Fig. 2).

For MMD-mixing (Def. 5), we consider joint distributions of states over multiple points in time. Thus, we consider subtrajectories and hence, multiple points in time simultaneously. While the estimation is conceptually identical to what is described above, we require an appropriate kernel to extend the MMD to joint distributions. In particular, the kernel has to be powerful enough to determine joint independence, which is called \mathcal{I} -characteristic.

Theorem 3 (Szabó & Sriperumbudur (2018)). Assume k is a universal kernel. Then the tensor kernel $k^s = \otimes_{i=1}^s k$ is an \mathcal{I} -characteristic kernel.

For example, a squared exponential kernel on the compact state space S is universal. Due to the tensor construction, we naturally obtain weak MMD-mixing with respect to k for an MMD-mixing process with respect to k^s . Thus, by considering a strong base kernel k , we can generalize our results. Strictly speaking, we require joint independence between all considered sample points to apply kernel two-sample tests. Thus, we need to extend our arguments to generalizations of the HSIC. The dHSIC (Pfister et al., 2016), for instance, yields a joint independence test. Thus, we can obtain a time shift a that yields joint independence by applying the dHSIC and leveraging the tensor kernel construction. The joint independence arguments apply to both MMD-mixing and weak MMD-mixing. Effectively, this results in more involved tensor kernel constructions that allow us to embed multiple joint probability distributions simultaneously. In practice, mixing is usually exponentially fast in the gap a . In all of our numerical experiments it was sufficient to estimate a single time shift a^* in the weak MMD-mixing sense.

5.3. Main Result

Next, we state our main result: a kernel two-sample test for dynamical systems. Due to MMD-mixing, waiting between consecutive samples yields arbitrarily small dependence in the data. For $a \rightarrow \infty$, we recover the i.i.d. setting. We state the asymptotic result based on Gretton et al. (2012a).

Proposition 1. Assume $\{X_k\}$ and $\{Y_k\}$ are stationary, ergodic, and MMD-mixing dynamical systems with distributions $\mathbb{P}_X, \mathbb{P}_Y$. Further, assume data $X_{a^*}, X_{2a^*}, \dots, X_{na^*}$ and $Y_{a^*}, Y_{2a^*}, \dots, Y_{na^*}$ is sampled i.i.d. from \mathbb{P}_X and \mathbb{P}_Y , respectively. If we obtain for the empirical estimate (4) that

$$\text{MMD}_b^2[\mathbb{P}_X, \mathbb{P}_Y] > \kappa(n, \alpha), \quad (8)$$

where κ is the threshold of the kernel-two sample test with significance α , then we can conclude that $\mathbb{P}_X \neq \mathbb{P}_Y$ with high probability $1 - \alpha$.

Proof. Essentially, we leverage the introduced notion of MMD-mixing to enforce independent data samples. Once we mitigate the correlations, we are comparing i.i.d. random variables and thus, can apply Gretton et al. (2012a), which gives us guarantees on the speed of convergence of (4) and thus, high confidence threshold κ for the test. \square

Remark 1. In practice, the autocorrelations will always be greater than zero. Also, it is important that either both systems have the same mixing speed or a^* corresponds to the slower system. Empirically, we can control the dependence and make it arbitrarily small by increasing the time shift a . By adapting the concentration results inside the kernel two-sample test, i.e., McDiarmid’s inequality, we can directly embed significant autocorrelations in the test statistic and potentially be more data-efficient. These results, however, would require further technical assumptions (cf. Assumption 3.1. in (Chérief-Abdellatif & Alquier, 2019)) and are left for future work. Here, we focus on introducing an efficient, sound, and practically relevant statistical test for dynamical systems.

5.4. Partially Observable Systems

In practice, we usually do not have access to the full state X_k . Instead we receive measurements $X'_k = g(X_k) + \xi_k$, where g is an observation function and $\xi_k \stackrel{\text{iid}}{\sim} \mathbb{P}_\xi$ measurement noise. Intuitively, the function g could be regarded as sensors that measure some quantity that depends on the underlying system. Thus, we could also infer different systems when, e.g., the measurement noise or the sensors are different. Further, it is not always possible to reconstruct the state, and appropriate observability assumptions would be required for this. However, this is not due to our test but an issue of the problem itself since the true underlying state is unknown. Nonetheless, we are able to apply the proposed test to measurements X'_k by considering the pushforward of the measure $g(\mathbb{P}_X)$ together with \mathbb{P}_ξ .

Proposition 2. Assume the same setting as in Proposition 1, however, with noisy measurements $X'_k = g(X_k) + \xi_k$ and $Y'_k = g(Y_k) + \xi_k$. If $\text{MMD}_b^2[\mathbb{P}_{X'}, \mathbb{P}_{Y'}] > \kappa(n, \alpha)$, then we conclude that $\mathbb{P}_{X'} \neq \mathbb{P}_{Y'}$ with high probability.

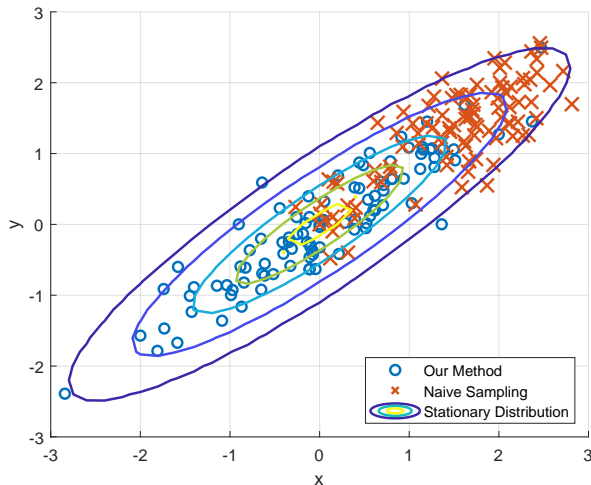


Figure 1. Scatter plot of an illustrative 2-dimensional LTI system. The system was designed to yield slow mixing times and initialized at $X_0 = 0$. The red crosses represent the first 100 states X_0, X_1, \dots, X_{100} . The blue circles represent states with an enforced time shift of $a^* = 75$ between samples. The stationary distribution of the system is illustrated as a contour plot.

In general, it is not clear what states to choose for an appropriate representation of a dynamical system, e.g., to model human walking. If we obtain rich information through sensor measurements then this is usually sufficient for subsequent downstream tasks (cf. Section 7).

6. Illustrative Examples

In this section, we illustrate two critical properties of our method: i) respecting the estimated time shift a^* yields samples whose distribution is indistinguishable from the stationary distribution, ii) violating the estimated time shift a^* leads to clustering effects that skew and bias the empirical distributions. More details to all of the mentioned experiments are provided in the supplementary material.

6.1. Linear Time-invariant System

Linear time-invariant (LTI) systems are prevalent in control and systems theory due to many analytically tractable properties. In particular, we can explicitly determine the stationary distribution (cf. supplementary material) and, thus, draw i.i.d. samples. Consider the dynamics

$$X_{k+1} = AX_k + \epsilon_k, \quad (9)$$

where $\epsilon_k \stackrel{\text{iid}}{\sim} \mathcal{N}(0, \Sigma)$. Further, assume all eigenvalues of $A \in \mathbb{R}^{d \times d}$ are located within the unit circle and $x_0 = 0$ to avoid potential transient behavior. We can now quantify the speed of mixing directly through the eigenvalues of A and Σ . If A has eigenvalues close to the boundary of the unit sphere, then this results in slow mixing. The same holds for

small process noise. On the contrary, small eigenvalues of A and large noise result in rapid mixing. An intuitive corner case is $A = 0$, which yields perfectly independent samples.

In Fig. 1, we illustrate the behavior of a two-dimensional slowly mixing system (9). In red, we plot the first 100 states of the systems, and in blue, states with an enforced time shift of $a^* = 75$ between consecutive samples. The estimated time shift $a^* = 75$ is obtained in the weak MMD-mixing sense as described in Sec. 5.2 and ensures that the HSIC is below the test threshold (cf. supplementary material). Further, we show a contour plot of the stationary distribution. Samples that were drawn based on our method coincide with the stationary distribution. The first 100 states, on the other hand, cluster in one region of the state space and are subject to heavy auto-correlations. The red crosses are clearly not representative of the stationary distribution.

To investigate this further, we applied kernel two-sample tests to distinguish between samples that are directly drawn from the stationary distribution and based on our method. Essentially, this turned out to be impossible since we recover the i.i.d. setting (cf. supplementary material).

We want to emphasize that mixing can be arbitrarily slow. In particular, it is possible that the system does not mix at all (Simchowitz et al., 2018). With the proposed method, we would notice this since we would not be able to estimate an a^* . Thus, we can decide whether the kernel two-sample test is applicable or not. We have also constructed non-mixing examples and obtained a constant HSIC that does not decrease over time (cf. supplementary material).

6.2. Lorenz Attractor

The Lorenz attractor is a famous chaotic and deterministic dynamical system. It is known to mix in a topological sense (Luzzatto et al., 2005). In the supplementary material, we provide empirical evidence that the Lorenz system mixes with respect to the herein introduced notion of MMD-mixing. Further, we can distinguish between two systems with slightly different parameters.

7. Experimental Example – Human Walking

We apply the developed kernel two-sample test to real-world experimental data that will be made available. We consider gait data of human subjects walking on a treadmill. Detecting characteristics and abnormalities in human gait is a highly relevant problem in disease prediction, diagnosis and progress monitoring as well as in biometrics (Nguyen et al., 2019; Gaßner et al., 2020; Muro-De-La-Herran et al., 2014). An example data set with a known ground truth label is obtained by letting subjects walk with and without a knee orthosis. Our goal is to classify each measured trajectory correctly with the labels *orthosis* and *no orthosis*.

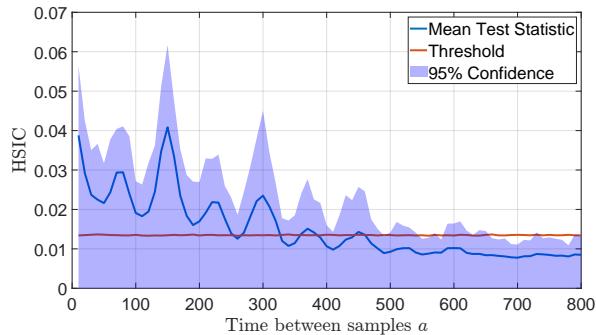


Figure 2. Mixing properties of gait data. On the x -axis, we depict the time shift a between consecutive samples. One time step corresponds to 0.01 seconds. The y -axis shows the dependence between data points with respect to the corresponding time shift. The initial point is randomized, and the estimation is repeated 50 times. Depicted is the mean of the test statistic and the 95% upper confidence bound. We also show the threshold κ of the independence test. When the blue line is below the red line, it is not possible to infer statistical dependence between the data points.

7.1. Data Collection

The IMU data of foot motion were collected from 38 healthy subjects without any restrictions in gait or illnesses that affect their walking ability. The data collection was conducted in the movement analysis laboratory of one of the authors' universities on a Mercury Med treadmill. The IMU sensors were attached to the test subjects' shoes using velcro straps. The measurements were taken for 90 seconds each trial under the following conditions: walking at very slow (1.5 km h^{-1}), slow (3 km h^{-1}), slow with simulated gait pathology, and normal walking speed (5 km h^{-1}). For the simulated gait pathology, the mobility of the left knee joint was restricted using a knee orthosis, which was fixed in a neutral position to disable further extension or flexion of the joint. The subjects were asked to stand still with both feet next to each other for 3 seconds at the beginning and the end of each trial. Before the trials, the subjects were able to practice walking on the treadmill. They were allowed to use the handrail of the treadmill if necessary. For 3 subjects, the orthosis experiment could not be carried out. An approval from the local ethics committee was obtained.

7.2. Description of the Statistical Test

We consider the gyroscopic data of the left foot for 35 subjects. The gyroscopic data is three-dimensional and consist of roughly 14 000 data points per trajectory.

7.2.1. MIXING PROPERTIES

First, we quantify the mixing properties of human walking. We estimate weak MMD-mixing (cf. Sec. 5.2) by applying the HSIC to the 35 subjects. We consider the trials with

and without the orthosis simultaneously, which yields 70 independent trajectories. We draw an initial point X_k from a uniform distribution between $k = 2000$ and $k = 4000$ and fix that point for all trajectories. Afterward, we compute $\text{HSIC}(X_k, X_{k+a})$ for various values of a , which is depicted in Fig. 2. To exclude numerical artifacts, we repeat the estimation of the mixing properties 50 times with randomly chosen initial points.

7.2.2. CLASSIFICATION

We compare MMD-based classification against standard baselines for the 70 trajectories.

MMD-based classification: We choose one trajectory of interest, for which we forget the correct label, and separate it from all other trajectories, for which the correct label is known. We pick a random initial point X_0 uniformly distributed between $k = 2000$ and $k = 3000$. After time shifting the data with respect to a^* , we estimate the MMD (4) between the trajectory of interest and all other trajectories. Then, we use the label of the trajectory with the smallest MMD to the unlabeled trajectory. Intuitively, unrestricted trajectories look more similar among themselves than trajectories with a restricted knee, and vice versa.

Baseline: We compare the proposed approach to common baselines that are commonly used for classification of biomedical data (Bidabadi et al., 2019; Misgeld et al., 2015; Tien et al., 2010). We consider the following features:

- Maximum and minimum value of each dimension;
- The 4 largest frequencies based on a Fourier transform;
- The 2-norm over time and the state dimensions.

In total, this results in 19 features for each trajectory that are used to train linear classifiers – support vector machines (SVM) and logistic regression (LR). Further, we use a 3-fold cross-validation technique. We repeat the training also 1000 times and report the average accuracy and standard deviation in Table 1.

7.3. Results

Our empirical analysis reveals that human walking mixes with respect to weak MMD-mixing (cf. Sec. 5.2). Further, as illustrated in Fig. 2, we can effectively estimate the speed of mixing. After roughly five footsteps, the dependence of data to its past is mostly gone and we can treat data as independent.

For MMD-based classification, we use a time shift of $a^* = 400$. This results in 25 points per trajectory. A larger choice of a^* around 600 would be closer to our theoretical results. However, due to the limited amount of data, this would reduce the number of available samples even further.

We run all classification algorithm 1000 times and report

Table 1. Classification accuracy for labeling the trajectories correctly into the labels *orthosis* and *no orthosis*. Mean accuracy with standard deviation over 1000 repetitions.

Our method	SVM	LR
95.7% ± 2.4%	86.9% ± 4.4%	92.5% ± 3.2%

the average accuracy and standard deviation in Table 1. Our method achieves the best accuracy and we are able to classify 99.99% of the subjects with *no orthosis* correctly.

7.4. Discussion

The above results show that our proposed method works well on a practically relevant non-trivial problem and outperforms common baselines. We spent a reasonable amount of time on designing good features in the comparison. While the accuracy of the linear classifiers could potentially be improved by adding additional features, designing such features requires more insight into the problem and system properties, which is unavailable in many applications. In order to improve the accuracy of our method it would suffice to add more data (i.e., consider longer trajectories) and it can directly be applied to a range of similar problems.

Classification and clustering algorithms based on the MMD can be applied in more general settings (Jegelka et al., 2009). Thus, our proposed nearest-neighbor approach for dynamical systems should generalize to more sophisticated clustering algorithms, which could yield unprecedented insights into the behavior of complex dynamical systems.

8. Conclusion

We propose a novel type of mixing that enables comparing dynamical systems from data through kernel two-sample tests. The proposed method is straightforward to use, has only few parameters, and is model free. In particular, we are able to estimate the speed of mixing in a relevant norm, which is a relevant contribution in itself. The flexibility and relevance of the proposed method are demonstrated numerically and experimentally on raw IMU data. The presented results point to great potential, in particular for biomedical and engineering applications, which we plan to explore in future work. Further, there are several theoretical extensions that we want to address in the future, such as generalized concentration inequalities and transient properties.

References

- Bidabadi, S. S., Murray, I., Lee, G. Y. F., Morris, S., and Tan, T. Classification of foot drop gait characteristic due to lumbar radiculopathy using machine learning algorithms. *Gait & posture*, 71:234–240, 2019.
- Birkhoff, G. D. Proof of the ergodic theorem. *Proceedings of the National Academy of Sciences*, 17(12):656–660, 1931.
- Brunton, S. L., Brunton, B. W., Proctor, J. L., Kaiser, E., and Kutz, J. N. Chaos as an intermittently forced linear system. *Nature communications*, 8(1):1–9, 2017.
- Chazottes, J.-R. Fluctuations of observables in dynamical systems: from limit theorems to concentration inequalities. In *Nonlinear dynamics new directions*, pp. 47–85. Springer, 2015.
- Chérif-Abdellatif, B.-E. and Alquier, P. Finite sample properties of parametric mmd estimation: robustness to misspecification and dependence. *arXiv preprint arXiv:1912.05737*, 2019.
- Chwialkowski, K. and Gretton, A. A kernel independence test for random processes. In *International Conference on Machine Learning*, pp. 1422–1430, 2014.
- Chwialkowski, K. P., Sejdinovic, D., and Gretton, A. A wild bootstrap for degenerate kernel tests. In *Advances in Neural Information Processing Systems*, pp. 3608–3616, 2014.
- Doran, G., Muandet, K., Zhang, K., and Schölkopf, B. A permutation-based kernel conditional independence test. In *UAI*, pp. 132–141, 2014.
- Gaßner, H., Jensen, D., Marxreiter, F., Kletsch, A., Bohlen, S., Schubert, R., Muratori, L. M., Eskofier, B., Klucken, J., Winkler, J., et al. Gait variability as digital biomarker of disease severity in huntington’s disease. *Journal of neurology*, pp. 1–8, 2020.
- Gretton, A., Fukumizu, K., Teo, C. H., Song, L., Schölkopf, B., and Smola, A. J. A kernel statistical test of independence. In *Advances in Neural Information Processing Systems*, pp. 585–592, 2008.
- Gretton, A., Borgwardt, K. M., Rasch, M. J., Schölkopf, B., and Smola, A. A kernel two-sample test. *Journal of Machine Learning Research*, 13(Mar):723–773, 2012a.
- Gretton, A., Sejdinovic, D., Strathmann, H., Balakrishnan, S., Pontil, M., Fukumizu, K., and Sriperumbudur, B. K. Optimal kernel choice for large-scale two-sample tests. In *Advances in Neural Information Processing Systems*, pp. 1205–1213, 2012b.
- Hang, H., Steinwart, I., et al. A bernstein-type inequality for some mixing processes and dynamical systems with an application to learning. *The Annals of Statistics*, 45(2): 708–743, 2017.
- Hang, H., Steinwart, I., Feng, Y., and Suykens, J. A. Kernel density estimation for dynamical systems. *The Journal of Machine Learning Research*, 19(1):1260–1308, 2018.
- Hwangbo, J., Lee, J., Dosovitskiy, A., Bellicoso, D., Tsounis, V., Koltun, V., and Hutter, M. Learning agile and dynamic motor skills for legged robots. *Science Robotics*, 4(26):eaau5872, 2019.
- Ishikawa, I., Fujii, K., Ikeda, M., Hashimoto, Y., and Kawahara, Y. Metric on nonlinear dynamical systems with Perron-Frobenius operators. In *Advances in Neural Information Processing Systems*, pp. 2856–2866, 2018.
- Ishikawa, I., Tanaka, A., Ikeda, M., and Kawahara, Y. Metric on random dynamical systems with vector-valued reproducing kernel Hilbert spaces. *arXiv preprint arXiv:1906.06957*, 2019.
- Jegelka, S., Gretton, A., Schölkopf, B., Sriperumbudur, B. K., and Von Luxburg, U. Generalized clustering via kernel embeddings. In *Annual Conference on Artificial Intelligence*, pp. 144–152. Springer, 2009.
- Jeschke, S., Brecher, C., Meisen, T., Özdemir, D., and Eschert, T. Industrial Internet of Things and cyber manufacturing systems. In *Industrial Internet of Things*, pp. 3–19. Springer, 2017.
- Klus, S., Schuster, I., and Muandet, K. Eigendecompositions of transfer operators in reproducing kernel Hilbert spaces. *Journal of Nonlinear Science*, 30(1):283–315, 2020.
- Ljung, L. System identification. *Wiley Encyclopedia of Electrical and Electronics Engineering*, 2001.
- Lloyd, J. R. and Ghahramani, Z. Statistical model criticism using kernel two sample tests. In *Advances in Neural Information Processing Systems*, pp. 829–837, 2015.
- Long, M., Zhu, H., Wang, J., and Jordan, M. I. Deep transfer learning with joint adaptation networks. In *Proceedings of the 34th International Conference on Machine Learning-Volume 70*, pp. 2208–2217. JMLR. org, 2017.
- Lueken, M. J., Misgeld, B. J., and Leonhardt, S. Classification of spasticity affected emg-signals. In *2015 IEEE 12th International Conference on Wearable and Implantable Body Sensor Networks (BSN)*, pp. 1–6. IEEE, 2015.
- Luzzatto, S., Melbourne, I., and Paccaut, F. The Lorenz attractor is mixing. *Communications in Mathematical Physics*, 260(2):393–401, 2005.

- McDonald, D., Shalizi, C., and Schervish, M. Estimating beta-mixing coefficients. In *Proceedings of the Fourteenth International Conference on Artificial Intelligence and Statistics*, pp. 516–524, 2011.
- Mezic, I. On comparison of dynamics of dissipative and finite-time systems using Koopman operator methods. *IFAC-PapersOnLine*, 49(18):454–461, 2016.
- Misgeld, B. J., Lüken, M., Heitzmann, D., Wolf, S. I., and Leonhardt, S. Body-sensor-network-based spasticity detection. *IEEE journal of biomedical and health informatics*, 20(3):748–755, 2015.
- Muandet, K., Fukumizu, K., Sriperumbudur, B., and Schölkopf, B. Kernel mean embedding of distributions: A review and beyond. *Foundations and Trends® in Machine Learning*, 10(1-2):1–141, 2017.
- Muro-De-La-Herran, A., Garcia-Zapirain, B., and Mendez-Zorrilla, A. Gait analysis methods: An overview of wearable and non-wearable systems, highlighting clinical applications. *Sensors*, 14(2):3362–3394, 2014.
- Nguyen, A., Roth, N., Ghassemi, N., Hannink, J., Seel, T., Klucken, J., Gaßner, H., and Eskofier, B. Development and clinical validation of inertial sensor-based gait-clustering methods in parkinson’s disease. *Journal of NeuroEngineering and Rehabilitation*, 16(77):1–14, 2019.
- Pfister, N., Bühlmann, P., Schölkopf, B., and Peters, J. Kernel-based tests for joint independence. *arXiv preprint arXiv:1603.00285*, 2016.
- Qin, S. J. and Badgwell, T. A. A survey of industrial model predictive control technology. *Control engineering practice*, 11(7):733–764, 2003.
- Schluter, H., Solowjow, F., and Trimpe, S. Event-triggered learning for linear quadratic control. *IEEE Transactions on Automatic Control*, 2020.
- Schölkopf, B. and Smola, A. J. *Learning with kernels: support vector machines, regularization, optimization, and beyond*. MIT press, 2001.
- Schön, T. B., Wills, A., and Ninness, B. System identification of nonlinear state-space models. *Automatica*, 47(1): 39–49, 2011.
- Schoukens, J. and Ljung, L. Nonlinear system identification: A user-oriented road map. *IEEE Control Systems Magazine*, 39(6):28–99, 2019.
- Sejdicinovic, D., Sriperumbudur, B., Gretton, A., and Fukumizu, K. Equivalence of distance-based and rkhs-based statistics in hypothesis testing. *The Annals of Statistics*, pp. 2263–2291, 2013.
- Simchowitz, M., Mania, H., Tu, S., Jordan, M. I., and Recht, B. Learning without mixing: Towards a sharp analysis of linear system identification. *Conference on Learning Theory*, pp. 439–473, 2018.
- Simon-Gabriel, C.-J., Barp, A., and Mackey, L. Metrizing weak convergence with maximum mean discrepancies. *arXiv preprint arXiv:2006.09268*, 2020.
- Solowjow, F. and Trimpe, S. Event-triggered learning. *Automatica*, 117:109009, 2020.
- Sorocky, M. J., Zhou, S., and Schoellig, A. P. Experience selection using dynamics similarity for efficient multi-source transfer learning between robots. In *Proc. of the IEEE International Conference on Robotics and Automation*, 2020.
- Sriperumbudur, B. K., Gretton, A., Fukumizu, K., Schölkopf, B., and Lanckriet, G. R. Hilbert space embeddings and metrics on probability measures. *The Journal of Machine Learning Research*, 11:1517–1561, 2010.
- Steinwart, I. and Christmann, A. *Support Vector Machines*. Springer Science & Business Media, 2008.
- Szabó, Z. and Sriperumbudur, B. Characteristic and universal tensor product kernels. *Journal of Machine Learning Research*, 18:233, 2018.
- Tien, I., Glaser, S. D., and Aminoff, M. J. Characterization of gait abnormalities in parkinson’s disease using a wireless inertial sensor system. In *2010 Annual International Conference of the IEEE Engineering in Medicine and Biology*, pp. 3353–3356. IEEE, 2010.
- Tolstikhin, I., Bousquet, O., Gelly, S., and Schölkopf, B. Wasserstein auto-encoders. In *International Conference on Learning Representations (ICLR 2018)*. OpenReview.net, 2018.
- Umlauf, J. and Hirche, S. Feedback linearization based on Gaussian processes with event-triggered online learning. *IEEE Transactions on Automatic Control*, 2019.
- Vishwanathan, S., Smola, A. J., and Vidal, R. Binet-Cauchy kernels on dynamical systems and its application to the analysis of dynamic scenes. *International Journal of Computer Vision*, 73(1):95–119, 2007.
- Yu, B. Rates of convergence for empirical processes of stationary mixing sequences. *The Annals of Probability*, pp. 94–116, 1994.
- Zaremba, W., Gretton, A., and Blaschko, M. B-test: A non-parametric, low variance kernel two-sample test. In *Advances in Neural Information Processing Systems*, pp. 755–763, 2013.

Zhou, K. and Doyle, J. C. *Essentials of Robust Control*, volume 104. Prentice hall Upper Saddle River, NJ, 1998.

Appendix

A. LTI Systems

There are several aspects that we kept short in the main paper and address in the following. We consider the dynamics

$$X_{k+1} = AX_k + \epsilon_k, \quad (10)$$

where $\epsilon_k \stackrel{\text{iid}}{\sim} \mathcal{N}(0, \Sigma)$. Further, assume all eigenvalues of $A \in \mathbb{R}^{d \times d}$ are located within the unit circle.

Stationary Distribution: The stationary distribution of an LTI system is Gaussian with expected value zero. The Gaussian distribution follows from the Gaussian noise and linear structure of the system. The expected value can be computed by leveraging that all eigenvalues of A are located within the unit circle. Obtaining the variance is more involved. It can be expressed as the solution to the following Lyapunov equation in Z (Schluter et al., 2020, Equation 7):

$$AZA^\top - Z + \Sigma = 0, \quad (11)$$

where A is the system matrix and Σ the covariance matrix of the process noise.

A.1. Comparison to Stationary

We investigate if we can, based on a kernel two-sample test, distinguish between time shifted samples with respect to a^* and i.i.d. samples from the stationary distribution.

Setup: We create 500 randomly generated LTI systems with a random dimensionality between 1 and 100. For each system we create $m = 250$ independent trajectories and sample $n = 20\,000$ points for each trajectory. All systems are initialized in $X_0 = 0$ to avoid transient effects. The decay of dependence is quantified in the weak MMD-sense for one gap (cf. Sec. 5 of main paper). We use data from the end of the trajectory to avoid numerical artifacts.

Next, we describe how we generate the system matrices.

Sampling Σ : The entries for the covariance matrix are drawn from a standard multivariate normal distribution. Since the matrix is supposed to yield a covariance matrix, we require symmetry and positive definiteness. Thus, we denote Σ' as the matrix drawn from the normal distribution and define $\Sigma = 0.5(\Sigma' + \Sigma'^\top)^2$. To control the magnitude of noise, we scale the matrix with the largest eigenvalue of Σ .

Sampling A : The system matrix A is required to have eigenvalues within the unit sphere. To achieve this, we draw

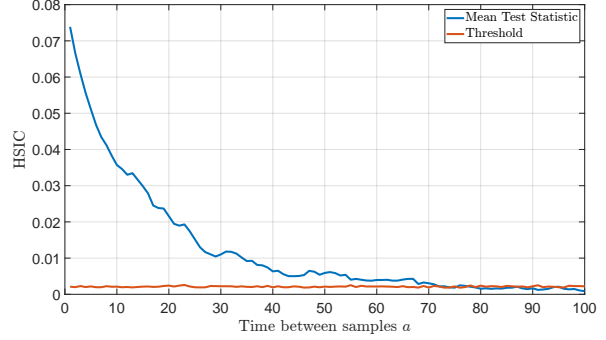


Figure 3. Mixing properties of the LTI system that is used to create Fig. 1 in the main paper. On the x -axis, we depict the time shift a between consecutive samples. The y -axis shows the dependence between data points with respect to the corresponding time shift. At $a^* = 75$ the test statistic is below the threshold.

the entries of A from a uniform distribution and extend the system with a control input

$$X_{k+1} = AX_k + Bu_k + \epsilon_k. \quad (12)$$

The control matrix B is set to the identity matrix and the control input as a standard linear quadratic feedback controller $u_k = -Kx_k$. This yields the closed loop dynamics

$$X_{k+1} = (A - BK)X_k + \epsilon_k. \quad (13)$$

The feedback gain K can be computed to minimize a linear quadratic cost function. By adjusting the weights of the cost function, we can indirectly adjust the eigenvalues of the closed loop system matrix $(A - BK)$. We set the weight matrix for the state cost Q to the identity matrix and the control cost to $R = 10^7$. This makes it very expensive to apply large control inputs and magnitude of the eigenvalues of $(A - BK)$ stays close to 1. This implies slow mixing and further, by considering $R \rightarrow \infty$, we can make this arbitrarily slow.

Results: First, we use the $m = 250$ trajectories to estimate the mixing speed a^* . We choose a^* as the first time instance at which the test statistic is below the test threshold.

For the kernel two-sample test, we draw 100 points from the first trajectory that respect the time shift a^* . We also draw 100 points directly from the stationary distribution ($\mathcal{N}(0, Z)$, cf. (11)).

From the 500 systems we considered overall, we only obtained 4 false positives, which shows the high precision of our proposed test. Due to the probabilistic nature of these experiments, we could obtain systems with arbitrarily slow mixing times and, subsequently, very long a^* . Thus, we decided to fix a maximum a^* as $a_{\max} = 200$, and ignore all systems with larger a^* . We obtained 81 systems that mix too slowly, i.e., $a^* > a_{\max}$.

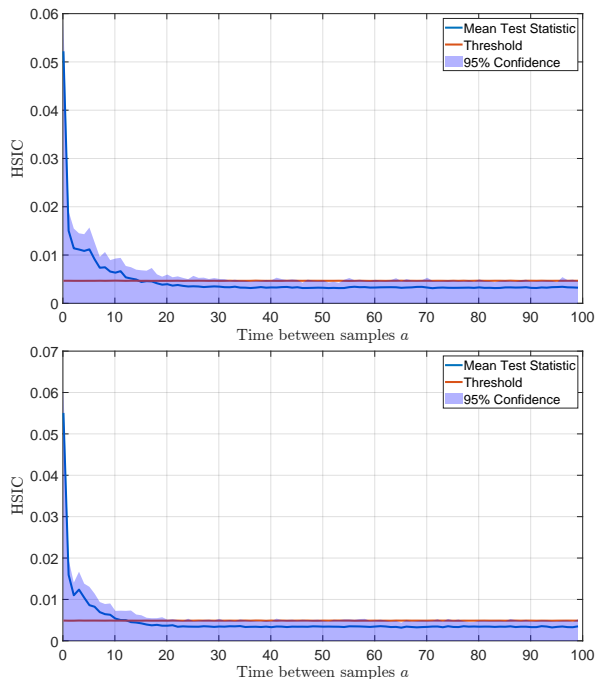


Figure 4. Mixing properties of the Lorenz system. Top plot with parameters as in (15)–(17) and below we adapted the parameter in (15) to 6. On the x -axis, we depict the time shift a between consecutive samples. The y -axis shows the dependence between data points with respect to the corresponding time shift. The initial point is randomized, and the estimation is repeated 100 times. Depicted is the mean of the test statistic and the 95% upper confidence bound. We also show the threshold κ of the independence test. When the blue line is below the red line, it is not possible to infer statistical dependence between the data points.

A.2. Details for Fig. 1 in the main paper:

In Fig. 3, we show the mixing properties of the system that yields $a^* = 75$. We used the same setup as in Sec. A.1 with some modifications. We chose $R = 10^{10}$ and divided Σ by $10\lambda_{\max}^2$, where λ_{\max} is the largest eigenvalue of Σ . Further, to be able to better visualize the samples and the stationary distributions, we fixed the dimension to two.

The randomly generated system matrices are

$$A = \begin{pmatrix} 0.2345 & 0.8609 \\ 0.7298 & 0.1316 \end{pmatrix}, \Sigma = \begin{pmatrix} 0.0378 & 0.0135 \\ 0.0135 & 0.0971 \end{pmatrix}. \quad (14)$$

B. Lorenz System

The classical Lorenz system is defined by the equations

$$\dot{x} = 10(y - x) \quad (15)$$

$$\dot{y} = 28x - y - xz \quad (16)$$

$$\dot{z} = xy - \frac{8}{3}z \quad (17)$$

and well investigated. To perform kernel two-sample testing, we slightly change the parameters in the Lorenz system by decreasing the coefficient in (15) from 10 to 6 to obtain a second slightly different system. The mixing analysis is done for both systems. The two systems are similar to each other, and yield similar looking attractors, which can be interpreted as the stationary probability distribution of the state.

B.1. Mixing properties

We estimate the mixing properties of the Lorenz system in the weak MMD-mixing sense for one time shift a (cf. Sec.5).

Initial points: We sample from an uniform distribution $\mathcal{U}([-0.5, 0.5] \times [-0.5, 0.5] \times [20, 21])$ to initialize the starting point X_0 .

Data: We use a standard ODE solver¹ to obtain a solution to the Lorenz system. Due to variable step sizes within the solver, we interpolate the solution to obtain samples with a fixed discretization in time. We consider the time horizon $t \in [0, 200]$ and create 2001 samples (with a fixed time step of 0.1).

Repetitions: We create $M = 100$ independent trajectories to estimate the mixing properties. The experiment is repeated $N = 100$ times to investigate deviations in the decay of the dependence.

Estimating mixing: To avoid numerical artifacts due to the initial points and potential transients, we consider data from the end of the trajectory. Thus, we sample at $t_{\text{end}} = 200$ and at $t - a$ for various values of $a = 0.1, 1.1, 2.1, \dots, 99.1$ with respect to the continuous time index t .

Results: We depict the decay of dependence in Fig. 4. After waiting for $a^* = 20$, the dependence in the data is not detectable anymore. Since the decay is not necessarily monotonic, we consider significantly higher time shifts up to $a = 99.1$. The dependence does not increase again, which indicates that the system is mostly mixing in the weak MMD-sense. Of course, this does not prove that the Lorenz system mixes and it remains to be shown rigorously. Nonetheless, these results are promising and provide empirical evidence.

B.2. Kernel Two-sample Test

We try to distinguish between the Lorenz system given in (15)–(17) and a slightly disturbed system where we change the parameter in (15) from 10 to 6. Based on the previous mixing analysis (cf. Fig. 4) we set the time shift $a^* = 20$. This yields approximately independent samples for both systems.

¹ode45 in Matlab

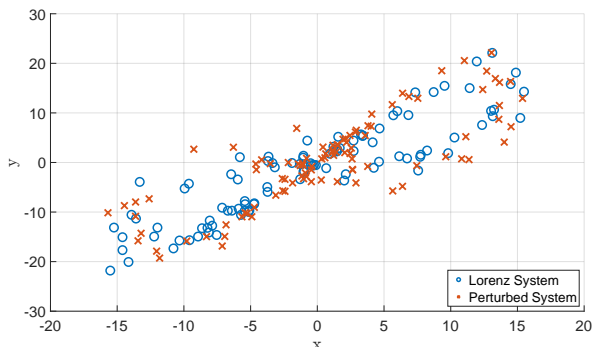


Figure 5. Scatter plot of the classical Lorenz system in blue circles (Eq. (15) – (17)) and the perturbed system in red crosses. Both systems are randomly initialized and sampled at time instances $t_1 = 20, t_2 = 40, \dots, t_{100} = 2000$.

We create two trajectories of different length t_{\max} and pick n points that respect the time shift a^* as illustrated in Fig. 5. We repeat all experiments 100 times. We start the sampling earliest at $t = 20$, which gives the system enough time to converge to the stationary distribution.

Accuracy: We use $t_{\max} = 6000$ and pick $n = 300$ points from both system. We achieve 95% accuracy in detecting different systems.

False positives: We consider two trajectories that were generated by the classical Lorenz system ((15) – (17)). The initial points for both trajectories were random and different. This setup yields 2.67% false positives, which is less than the α -level of 5% that we used.

Next, we investigate what happens if we violate a^* . We choose $n = 100$ and $t_{\max} = 30$. Thus, we sample 100 points in the time interval $t \in [20, 30]$. This clearly violates the estimated a^* and indeed, we obtain 51% false positives. Essentially, this makes the test useless when a^* is severely violated and thus, we want to emphasize again that it is critical to estimate a^* . Further, through an appropriate choice of a^* we inherit all the rich theoretical properties of kernel two-sample testing.

C. Non-mixing System

We construct a system that does not mix in the weak MMD sense and is also not expected to mix. However, the system is well known to be ergodic and stationary. In particular, we consider a dynamical system that moves on a circle with a radius of one and steps of length $\frac{\pi}{10}$. We create $m = 100$ randomly initialized points θ_0 and iterate them for $n = 100$ timesteps with the dynamics following

$$\theta_{k+1} = \theta_k + \frac{\pi}{10}, \quad (18)$$

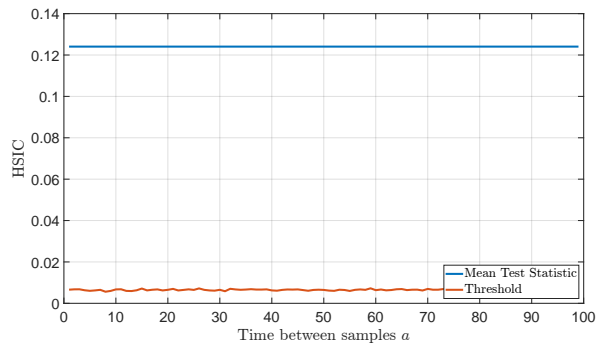


Figure 6. Mixing properties of a dynamical system that moves on a circle. The dependency between data points does not decrease and stays above the threshold.

and

$$X_{k+1} = \begin{pmatrix} \cos(\theta_k) \\ \sin(\theta_k) \end{pmatrix} \quad (19)$$

We show the mixing properties in Fig. 6. The dependence between data points stays constant and does not decrease and we detect this. Thus, we correctly identify systems that are not mixing in the MMD sense.

D. Implementations

Since our method is leveraging results from standard kernel two-sample testing and the HSIC, we directly used existing implementations without modifying them.

Kernel Two-sample Test Implementation: We used the Matlab implementation: <http://www.gatsby.ucl.ac.uk/~gretton/mmd/mmd.htm> and the standard hyperparameters without any tuning. We used the significance level $\alpha = 0.05$ for all experiments.

HSIC Implementation: We used the Matlab implementation: <http://people.kyb.tuebingen.mpg.de/arthur/indep.htm> with standard hyperparameters and $\alpha = 0.05$ for all experiments.